

Branched Luminescent Multinuclear Platinum(II) Alkynyl Complexes: Candidates for Efficient Two-Photon Induced Luminescence

Chi-Hang Tao,^{†,‡} Hui Yang,^{‡,§} Nianyong Zhu,^{†,‡} Vivian Wing-Wah Yam,^{*,†,‡} and Shi-Jie Xu^{*,‡,§}

Centre for Carbon-Rich Molecular and Nano-Scale Metal-Based Materials Research and Department of Chemistry, HKU-CAS Joint Laboratory on New Materials, and Department of Physics, The University of Hong Kong, Pokfulam Road, Hong Kong, People's Republic of China

Received April 16, 2008

Three luminescent multinuclear platinum(II) alkynyl complexes with readily tunable emission characteristics are found to show two-photon absorption (TPA) and two-photon induced luminescence (TPIL) properties, and their two-photon absorption cross-sections have been determined.

Introduction

Two-photon absorption (TPA) takes place when a molecule is excited from the ground state to an excited state by simultaneous absorption of two photons, while two-photon induced luminescence (TPIL) is the emission of light with energy higher than that of the absorbed light via two-photon absorption processes. Practical applications based on TPA have been rather limited in the past. It has only been since the mid 1990s, when advances in high-power lasers and the availability of materials with large TPA become more apparent, that there has been increasing attention devoted to TPA-based applications in photonic and biophotonic areas, such as optical data storage,^{1–3} power limiting,^{4,5} upconversion lasing,^{6,7} three-dimensional fluorescence imaging,^{8,9} three-dimensional micro-fabrication,^{10,11} pulse reshaping and stabilization,¹² and photodynamic therapy.^{13,14} Extensive efforts have been concentrated on the synthesis of organic chromophores with large two-photon absorption cross-section (σ_2) values.^{15–18} It has been reported that π -conjugated molecules that undergo large changes in

quadrupole moment upon excitation can show large two-photon absorption cross-sections.¹⁷ In particular, compounds with donor– π –donor, donor–acceptor–donor, and acceptor–donor–acceptor structural motifs could exhibit large σ_2 values.¹⁷ In addition, multibranching and dendritic systems with various structural motifs, such as 4,4',4''-trisubstituted triphenylamine,^{15,19} 1,3,5-tricyanobenzene,²⁰ 1,3,5-trisubstituted benzene,²¹ truxene,²² and others,²³ are also reported to show exceptionally large σ_2 values. These molecular design strategies have been proven to be useful in the preparation of novel materials with large two-photon absorption cross-sections.

In contrast, upconversion of light using d-block transition-metal complexes is relatively uncommon and most of the species used are coordination compounds.^{4,24–26} In fact, the incorporation of electron-donor or -acceptor moieties through the formation of relatively strong M–C bonds appears to be an attractive and promising strategy toward molecular materials with nonlinear optical properties. For instance, a number of ferrocenyl,

* To whom correspondence should be addressed. Fax: 852 2857 1586 (V.W.-W.Y.); 852 2559 9152 (S.-J.X.). Tel: 852 2859 2153 (V.W.-W.Y.); 852 2241 5636 (S.-J.X.). E-mail: wwyam@hku.hk (V.W.-W.Y.); sjxu@hkuc.hku.hk (S.-J.X.).

[†] Centre for Carbon-Rich Molecular and Nano-Scale Metal-Based Materials Research and Department of Chemistry.

[‡] HKU-CAS Joint Laboratory on New Materials.

[§] Department of Physics.

- (1) Strickler, J. H.; Webb, W. W. *Adv. Mater.* **1993**, *5*, 479.
- (2) Parthenopoulos, D. A.; Rentzepis, P. M. *Science* **1999**, *245*, 843.
- (3) He, G. S.; Gvishi, R.; Prasad, P. N.; Reinhardt, B. *Opt. Commun.* **1995**, *117*, 133.
- (4) Perry, J. W.; Mansour, K.; Lee, I.-Y. S.; Wu, X.-L.; Bedworth, P. V.; Chen, C.-T.; Ng, D.; Marder, S. R.; Miles, P.; Wada, T.; Tian, M.; Sasabe, H. *Science* **1996**, *273*, 1533.
- (5) He, G. S.; Xu, G. C.; Prasad, P. N.; Reinhardt, B. A.; Bhatt, J. C.; Dillard, A. G. *Opt. Lett.* **1995**, *20*, 435.
- (6) Mukherjee, A. *Appl. Phys. Lett.* **1993**, *62*, 3423.
- (7) Zheng, Q.; He, G. S.; Lin, T.-C.; Prasad, P. N. *J. Mater. Chem.* **2003**, *13*, 2499.
- (8) Belfield, K. D.; Schafer, K. J.; Liu, Y.; Liu, J.; Ren, X.; Van Stryland, E. W. *J. Phys. Org. Chem.* **2000**, *13*, 837.
- (9) Gu, M.; Tannous, T.; Sheppard, C. J. R. *Opt. Commun.* **1995**, *117*, 406.
- (10) Wang, X. L.; Krebs, J.; Al-Nuri, M. H.; Pudavar, E.; Ghosal, S.; Liebow, C.; Nagy, A. A.; Schally, A. V.; Prasad, P. N. *Proc. Natl. Acad. Sci. U.S.A.* **1999**, *96*, 11081.
- (11) Maruo, S.; Nakamura, O.; Kawata, S. *Opt. Lett.* **1997**, *22*, 132.

(12) He, G. S.; Yuan, L.; Bhawalkar, J. D.; Prasad, P. N. *Appl. Opt.* **1997**, *36*, 3387.

(13) Bhawalkar, J. D.; Kumar, N. D.; Zhao, C. F.; Prasad, P. N. *J. Clin. Med. Surg.* **1997**, *37*, 510.

(14) Frederiksen, P. K.; Jørgensen, M.; Ogilby, P. R. *J. Am. Chem. Soc.* **2001**, *123*, 1215.

(15) Marder, S. R. *Chem. Commun.* **2006**, 131.

(16) Huang, Z.-L.; Lei, H.; Li, N.; Qiu, Z. R.; Wang, H.-Z.; Guo, J.-D.; Luo, Y.; Zhong, Z.-P.; Liu, X.-F.; Zhou, Z.-H. *J. Mater. Chem.* **2003**, *13*, 708.

(17) Albota, M.; Beljonne, D.; Brédas, J.-L.; Ehrlich, J. E.; Fu, J.-Y.; Heikal, A. A.; Hess, S. E.; Kogej, T.; Levin, M. D.; Marder, S. R.; McCordMaughon, D.; Perry, J. W.; Röckel, H.; Rumi, M.; Subramaniam, G.; Webb, W. W.; Wu, X.-L.; Wu, C. *Science* **1998**, *281*, 1653.

(18) Reinhardt, B. A.; Brott, L. L.; Clarkson, S. J.; Dillard, A. G.; Bhatt, J. C.; Yuan, L.; He, G. S.; Prasad, P. N. *Chem. Mater.* **1998**, *10*, 1863.

(19) Lee, H. J.; Sohn, J.; Hwang, J.; Park, S. Y.; Choi, H.; Cha, M. *Chem. Mater.* **2004**, *16*, 456.

(20) Cho, B. R.; Son, K. H.; Lee, S. H.; Song, Y.-S.; Lee, Y.-K.; Jeon, S.-J.; Choi, J. H.; Lee, H.; Cho, M. *J. Am. Chem. Soc.* **2001**, *123*, 10039.

(21) Kato, S.-i.; Matsumoto, T.; Shigeiwa, M.; Gorohmaru, H.; Shuichi, M.; Ishii, T.; Mataka, S. *Chem. Eur. J.* **2006**, *12*, 2303.

(22) Zheng, Q.; He, G. S.; Prasad, P. N. *Chem. Mater.* **2005**, *17*, 6004.

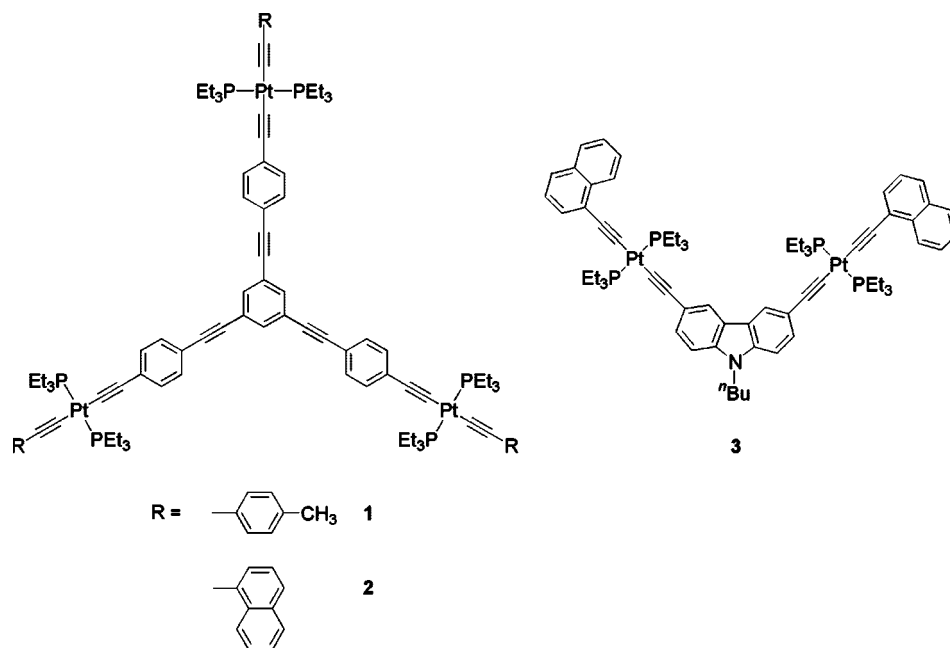
(23) He, G. S.; Tan, L.-S.; Zheng, Q.; Prasad, P. N. *Chem. Rev.* **2008**, *108*, 1245, and references therein.

(24) Zheng, Q.; He, G. S.; Prasad, P. N. *J. Mater. Chem.* **2005**, *15*, 579.

(25) Briñas, R. P.; Troxler, T.; Hochstrasser, R. M.; Vinogradov, S. A. *J. Am. Chem. Soc.* **2005**, *127*, 11851.

(26) Das, S.; Nag, A.; Goswami, D.; Bharadwaj, P. K. *J. Am. Chem. Soc.* **2006**, *128*, 402.

Chart 1. Structures of the Platinum Complexes



manganese(I), ruthenium(II), and gold(I) organotransition-metal complexes have been studied by various groups and are found to have interesting nonlinear optical responses.^{27–34} The platinum(II) alkynyl polymers and molecular materials represent one of the recent foci for the study of metal-containing NLO materials due to their strong excited-state absorptions in the visible range and relatively large spin–orbit coupling.^{35–42} Their negligible absorption in the visible region have rendered them as promising optical limiters in the visible region.^{39,41,43,44} Most of these materials are mononuclear platinum(II) complexes that

are structurally related to bis((4-(phenylethynyl)phenyl)ethynyl)bis(tributylphosphine)platinum(II), with reported σ_2 values in the range of ~ 5 – 10 GM, and their luminescence is reported as originating from the singlet or triplet excited state of the (4-(phenylethynyl)phenyl)ethynyl backbone.^{36–38,40} Incorporation of electron-donating or -accepting functionalities into this class of complexes for the enhancement of σ_2 values has been recently demonstrated.^{38–40} Although dendrimer-encapsulated derivatives of bis((4-(phenylethynyl)phenyl)ethynyl)bis(tributylphosphine)platinum(II) have also been reported,³⁷ the use of multinuclear platinum(II) alkynyls with dendritic or branched phenyleneethynylene backbones in the field of NLO studies has been largely neglected,^{40,44} in spite of the potential advantages of branched molecules and dendrimers, which is in contrast to the extensive studies of dendritic or branched compounds in organic NLO materials.²³ With our recent work and ongoing interest in the synthesis of luminescent branched alkynyls with various metal centers,^{45–49} we became interested in the exploration of these branched metal complexes as molecular materials with relatively efficient TPA and TPIL capabilities. These branched materials also possess better solubilities and processabilities in comparison to those of their linear counterparts, which may be advantageous for future applications. We are also interested in the effect on NLO properties of these metal-containing carbon-rich materials by changing the emission origin from the 4-(phenylethynyl)phenylethynyl backbone to a more low-lying moiety. In this regards, three multinuclear branched platinum(II) alkynyl complexes with two-photon induced luminescence properties are reported and their structures are shown in Chart 1.

(27) Green, M. L. H.; Marder, S. R.; Thompson, M. E.; Bandy, J. A.; Bloor, D.; Kolinsky, P. V.; Jones, R. J. *Nature* **1987**, *330*, 360.

(28) Green, M. L. H.; Qin, J.; O'Hare, D.; Bunting, H. E.; Thompson, M. E.; Marder, S. R.; Chatakondou, K. *Pure Appl. Chem.* **1989**, *61*, 817.

(29) Bunting, H. E.; Green, M. L. H.; Marder, S. R.; Thompson, M. E.; Bloor, D.; Kolinsky, P. V.; Jones, R. J. *Polyhedron* **1992**, *11*, 1489.

(30) Bandy, J. A.; Bunting, H. E.; Garcia, M. H.; Green, M. L. H.; Marder, S. R.; Thompson, M. E.; Bloor, D.; Kolinsky, P. V.; Jones, R. J.; Perry, J. W. *Polyhedron* **1992**, *11*, 1429.

(31) Barlow, S.; Marder, S. R. *Chem. Commun.* **2000**, 1555, and references therein.

(32) Davies, S. J.; Johnson, B. F. G.; Lewis, J.; Khan, M. S. J. *Organomet. Chem.* **1991**, *401*, C43.

(33) Colbert, M. C. B.; Edwards, A. J.; Lewis, J.; Long, N. L.; Page, N. A.; Parker, D. G.; Raithby, P. R. *J. Chem. Soc., Dalton Trans.* **1994**, *17*, 2589.

(34) Cifuentes, M. P.; Humphrey, M. G. *J. Organomet. Chem.* **2004**, *689*, 3968.

(35) McKay, T. J.; Bolger, J. A.; Staromlynska, J.; Davy, J. R. *J. Chem. Phys.* **1998**, *108*, 5537.

(36) McKay, T. J.; Staromlynska, J.; Wilson, P.; Davy, J. *J. Appl. Phys.* **1999**, *85*, 1337.

(37) Vestberg, R.; Westlund, R.; Eriksson, A.; Lopes, C.; Carlsson, M.; Eliasson, B.; Glimsdal, E.; Lindgren, M.; Malmström, E. *Macromolecules* **2006**, *39*, 2238.

(38) Glimsdal, E.; Carlsson, M.; Eliasson, B.; Minaev, B.; Lindgren, M. *J. Phys. Chem. A* **2007**, *111*, 244.

(39) Lind, P.; Boström, D.; Carlsson, M.; Eriksson, A.; Glimsdal, E.; Lindgren, M.; Eliasson, B. *J. Phys. Chem. A* **2007**, *111*, 1598.

(40) Rogers, J. E.; Slagle, J. E.; Krein, D. M.; Burke, A. R.; Hall, B. C.; Fratini, A.; McLean, D. G.; Fleitz, P. A.; Cooper, T. M.; Drobizhev, M.; Makarov, N. S.; Rebane, A.; Kim, K.-Y.; Farley, R.; Schanze, K. S. *Inorg. Chem.* **2007**, *46*, 6483.

(41) Westlund, R.; Glimsdal, E.; Lindgren, M.; Vestberg, R.; Hawker, C.; Lopes, C.; Malmström, E. *J. Mater. Chem.* **2008**, *18*, 166.

(42) D'Amato, R.; Furlani, A.; Colapietro, M.; Portalone, G.; Casalboni, M.; Falconieri, M.; Russo, M. V. *J. Organomet. Chem.* **2001**, *627*, 13.

(43) Staromlynska, J.; McKay, T. J.; Wilson, P. *J. Appl. Phys.* **2000**, *88*, 1726.

(44) Desroches, C.; Lopes, C.; Kessler, V.; Parola, S. *Dalton Trans.* **2003**, 2085.

(45) Yam, V. W.-W. *Acc. Chem. Res.* **2002**, *35*, 555.

(46) Tao, C. H.; Zhu, N.; Yam, V. W.-W. *Chem. Eur. J.*, **2005**, *11*, 1647; **2008**, *14*, 1377.

Experimental Section

Materials and Reagents. $[\{RC\equiv C(PEt_3)_2PtC\equiv CC_6H_4C\equiv C\}_3-C_6H_3-1,3,5]$ (R = C₆H₄CH₃ (**1**), Np (**2**))⁴⁶ and the precursor complex $[\{ClPt(PEt_3)_2C\equiv C\}_2-3,6-{}^tBuCarb-9]$ ⁵⁰ were synthesized according to literature procedures. 1-Ethynyl naphthalene (Aldrich, 97%) was purchased and used as received. All amines were distilled over potassium hydroxide and stored in the presence of potassium hydroxide prior to use. All other solvents and reagents were of analytical grade and were used as received.

Physical Measurements and Instrumentation. UV–visible spectra were obtained on a Hewlett-Packard 8452A diode array spectrophotometer, IR spectra as KBr disks on a Bio-Rad FTS-7 Fourier transform infrared spectrophotometer (4000–400 cm⁻¹), and steady-state excitation and emission spectra on a Spex Fluorolog-2 Model F 111 fluorescence spectrophotometer equipped with a Hamamatsu R-928 photomultiplier tube. Low-temperature (77 K) spectra were recorded by using an optical Dewar sample holder. ¹H NMR spectra were recorded on a Bruker DPX-300 Fourier transform NMR spectrometer, while ³¹P{¹H} NMR spectra were recorded on either a Bruker DPX-300 or a Bruker DPX-500 Fourier transform NMR spectrometer. Chemical shifts (δ , ppm) of ¹H NMR spectra were recorded relative to tetramethylsilane (Me₄Si), while those of ³¹P NMR spectra were recorded relative to 85% H₃PO₄. Positive ion FAB mass spectra were recorded on a Finnigan MAT95 mass spectrometer. Elemental analyses of the new complexes were performed on a Carlo Erba 1106 elemental analyzer at the Institute of Chemistry, Chinese Academy of Sciences.

The two-photon induced luminescence measurements were performed with a mode-locked femtosecond Tsunami Ti:Sapphire laser (Spectra-Physics, 100 fs, 82 MHz) as a pump source. The tunable wavelength range of the pulses was 700–900 nm. The luminescence signals from both the solution and solid-state samples were collected at right angles to the samples with a pair of lenses and were dispersed with an Acton SP300 monochromator equipped with a photomultiplier (Hamamatsu R928) detector. A blue band color filter was used to block the laser line. A standard lock-in amplification technique was employed for the photoluminescence measurements. In the experiment, the two-photon absorption cross-section at 740 nm and the luminescence quantum yield of rhodamine 6G in methanol were assumed to be 20 GM (Göppert-Mayer, 1 GM = 1 × 10⁻⁵⁰ cm⁴ s photon⁻¹ molecule⁻¹) and 0.98,⁵¹ respectively. The time-averaged laser power at 740 nm was kept constant for the sample and the reference. For power-dependent measurements, the intensity of the incident laser was controlled with a neutral-density metallic filter.

All solutions for photophysical and two-photon induced luminescence studies were degassed on a high-vacuum line in a two-compartment cell consisting of a 10 mL Pyrex bulb and a 1 cm path length quartz cuvette and sealed from the atmosphere by a Bibby Rotaflo HP6 Teflon stopper. The solutions were subjected to at least four freeze–pump–thaw cycles. Thin-film solid-state two-photon induced luminescence measurements were carried out with solid samples dissolved in dichloromethane and casted onto a quartz plate.

(47) Yam, V. W.-W.; Tao, C. H.; Zhang, L.; Wong, K. M.-C.; Cheung, K.-K. *Organometallics* **2001**, *20*, 453.

(48) Chong, S. H.-F.; Lam, S. C.-F.; Yam, V. W.-W.; Zhu, N.; Cheung, K.-K. *Organometallics* **2004**, *23*, 4924.

(49) Lu, X.-X.; Li, C.-K.; Cheng, E. C.-C.; Zhu, N.; Yam, V. W.-W. *Inorg. Chem.* **2004**, *43*, 2225.

(50) Tao, C. H.; Wong, K. M.-C.; Zhu, N.; Yam, V. W.-W. *New J. Chem.* **2003**, *27*, 150.

(51) Albot, M. A.; Xu, C.; Webb, W. W. *Appl. Opt.* **1998**, *37*, 7352.

(52) Otwinowski, Z.; Minor, W. In *Macromolecular Crystallography Part A*; Carter, C. W., Sweet, R. M., Jr., Eds.; Academic Press: New York, 1997; Methods in Enzymology Part A, Vol. 276, pp 307–326.

(53) Sheldrick, G. M. *SHELXS97, Programs for Crystal Structure*; University of Göttingen, Göttingen, Germany, 1997.

Crystal Structure Determination. Single crystals of **3** were grown by the slow evaporation of a dichloromethane–methanol solution containing the complex. Crystal data for **3**: [C₆₈H₈₉NP₄Pt₂], formula weight 1434.46, monoclinic, space group *P2₁/c*, *a* = 22.582(4) Å, *b* = 10.013(2) Å, *c* = 28.585(6) Å, β = 91.91(3)°, *V* = 6460(2) Å³, *Z* = 4, *D_c* = 1.475 g cm⁻³, μ (Mo K α) = 4.464 mm⁻¹, *F*(000) = 2880, *T* = 253 K. A crystal of dimensions 0.40 mm × 0.20 mm × 0.15 mm mounted in a glass capillary was used for data collection at 253 K on a MAR diffractometer with a 300 mm image plate detector using graphite-monochromated Mo K α radiation (λ = 0.71073 Å). Data collection was made with 2° oscillation steps of φ , 10 min exposure time, and a scanner distance at 120 mm. A total of 100 images was collected. The images were interpreted and intensities integrated using the DENZO program.⁵² The structure was solved by direct methods employing the SHELXS-97 program⁵³ on a PC. Pt, P, and most non-hydrogen atoms were located according to direct methods. The positions of the other non-hydrogen atoms were found after successful refinement by full-matrix least squares using the SHELXL-97 program⁵⁴ on a PC. Restraints were applied to the ^tBu group, assuming similar C–C bond lengths. According to the SHELXL-97 program,⁵⁴ all 8716 independent reflections (*R_{int}* equal to 0.0617, 4350 reflections larger than 4 σ (*F_o*), where $R_{int} = \sum [F_o^2 - F_o^2(\text{mean})] / \sum [F_o^2]$) from a total of 27 496 reflections participated in the full-matrix least-squares refinement against *F*². These reflections were in the ranges $-25 \leq h \leq 24$, $-11 \leq k \leq 10$, and $-33 \leq l \leq 32$ with $2\theta_{max}$ equal to 50.56°. One crystallographic asymmetric unit consists of one formula unit. In the final stage of least-squares refinement, all non-hydrogen atoms were refined anisotropically. The hydrogen atoms were generated by the SHELXL-97 program.⁵⁴ The positions of hydrogen atoms were calculated on the basis of the riding mode with thermal parameters equal to 1.2 times that of the associated C atoms and participated in the calculation of final *R* indices. Since the structure refinements are against *F*², *R* indices based on *F*² are larger than (more than double) those based on *F*. For comparison with older refinements based on *F* and an OMIT threshold, a conventional index *R*1 based on observed *F* values larger than 4 σ (*F_o*) is also given (corresponding to (intensity)2 σ (*I*)). $wR2 = \{\sum [w(F_o^2 - F_c^2)^2] / \sum [w(F_o^2)^2]\}^{1/2}$; $R1 = \sum |F_o| - |F_c| / \sum |F_o|$. The goodness of fit is based on *F*²: $GOF = S = \{\sum [w(F_o^2 - F_c^2)^2] / (n - p)\}^{1/2}$, where *n* is the number of reflections and *p* is the total number of parameters refined. The weighting scheme is $w = 1/[\sigma^2(F_o^2) + (aP)^2 + bP]$, where *P* is $[2F_c^2 + \text{Max}(F_o^2, 0)]/3$. Convergence ((Δ / σ)_{max} = 0.001, average 0.001) for 676 variable parameters by full-matrix least-squares refinement on *F*² reaches to *R*1 = 0.0340 and *wR*2 = 0.0745 with a goodness of fit of 0.803; the parameters *a* and *b* for the weighting scheme are 0.0369 and 0.0, respectively. The final difference Fourier map shows maximum rest peaks and holes of 0.918 and $-0.638 \text{ e } \text{Å}^{-3}$, respectively.

Synthesis of Complex 3. All reactions were performed under anaerobic and anhydrous conditions using standard Schlenk techniques under an inert atmosphere of nitrogen. $[\{ClPt(PEt_3)_2C\equiv C\}_2-3,6-{}^tBuCarb-9]$ (200 mg, 0.166 mmol) and 1-ethynyl naphthalene (76 mg, 0.5 mmol) were dissolved in a mixture of THF (20 mL) and diethylamine (10 mL). To this reaction mixture was added CuCl (5 mg) as a catalyst. The yellow mixture was then stirred overnight at room temperature. The white organic ammonium salt that formed during the course of the reaction was filtered out and the solvent removed under reduced pressure. The resulting greenish yellow gummy residue was then redissolved in dichloromethane, and this solution was washed successively with brine and deionized water and dried over anhydrous Na₂SO₄. The solvent was then removed under reduced pressure. The yellow residue was subjected to column chromatography on basic aluminum oxide (50–200 μ m) using dichloromethane as the eluent. Yield: 131 mg, 55%. ¹H NMR

(54) Sheldrick, G. M. *SHELXL97, Programs for Crystal Structure*; University of Göttingen, Göttingen, Germany, 1997.

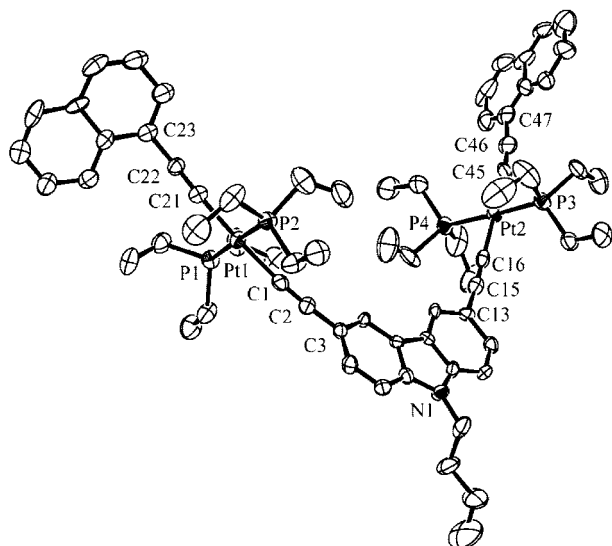


Figure 1. Perspective drawing of complex **3** with atomic numbering. Hydrogen atoms have been omitted for clarity. The thermal ellipsoids are shown at the 30% probability level.

Table 1. Selected Bond Distances (Å) and Bond Angles (deg) with Estimated Standard Deviations (Esd's) in Parentheses for Complex **3**

Bond Distances			
Pt(1)–C(21)	2.012(11)	Pt(2)–P(4)	2.299(3)
Pt(1)–C(1)	2.024(11)	Pt(2)–P(3)	2.308(3)
Pt(1)–P(1)	2.302(3)	C(1)–C(2)	1.208(13)
Pt(1)–P(2)	2.303(3)	C(15)–C(16)	1.239(14)
Pt(2)–C(16)	2.016(13)	C(21)–C(22)	1.177(12)
Pt(2)–C(45)	2.027(13)	C(45)–C(46)	1.218(17)
Bond Angles			
C(21)–Pt(1)–C(1)	176.4(4)	C(45)–Pt(2)–P(3)	92.8(3)
C(21)–Pt(1)–P(1)	92.2(3)	P(4)–Pt(2)–P(3)	175.36(11)
C(1)–Pt(1)–P(1)	88.9(3)	C(2)–C(1)–Pt(1)	175.5(10)
C(21)–Pt(1)–P(2)	89.3(3)	C(1)–C(2)–C(3)	175.9(12)
C(1)–Pt(1)–P(2)	89.6(3)	C(16)–C(15)–C(13)	172.9(11)
P(1)–Pt(1)–P(2)	178.30(11)	C(15)–C(16)–Pt(2)	177.3(10)
C(16)–Pt(2)–C(45)	179.0(4)	C(22)–C(21)–Pt(1)	176.9(10)
C(16)–Pt(2)–P(4)	90.5(3)	C(21)–C(22)–C(23)	175.8(12)
C(45)–Pt(2)–P(4)	88.7(3)	C(46)–C(45)–Pt(2)	174.9(12)
C(16)–Pt(2)–P(3)	87.9(3)	C(45)–C(46)–C(47)	170.6(17)

(CDCl₃, 298 K, 400 MHz): δ 0.93 (t, $J_{\text{HH}} = 6.8$ Hz, 3H, $-\text{NCH}_2\text{CH}_2\text{CH}_2\text{CH}_3$), 1.2–1.4 (m, 38H, $-\text{PCH}_2\text{CH}_3$ and $-\text{NCH}_2\text{CH}_2\text{CH}_2-$), 1.81 (quintet, $J_{\text{HH}} = 6.8$ Hz, 2H, $-\text{NCH}_2\text{CH}_2-$), 2.2–2.3 (m, 24H, $-\text{CH}_2\text{P}$), 4.22 (t, $J_{\text{HH}} = 6.8$ Hz, 2H, NCH_2-), 7.22 (d, $J_{\text{HH}} = 8.6$ Hz, 2H, H's at 1-position of carbazole), 7.3–7.5 (m, 10H, H's on Np moieties and H's at 2-position of carbazole), 7.63 (d, $J_{\text{HH}} = 8.1$ Hz, 2H, H's on Np moieties), 7.99 (d, $J_{\text{HH}} = 1.7$ Hz, 2H, H's at 4-position of carbazole), 8.54 (d, $J_{\text{HH}} = 8.1$ Hz, H's on Np moieties). $^{31}\text{P}\{^1\text{H}\}$ NMR (CDCl₃, 298 K, 162 MHz): δ 11.6 ($J_{\text{Pt-P}} = 2380$ Hz). IR (KBr disk, cm^{-1}): 2085 $\nu(\text{C}\equiv\text{C})$. Positive ion FAB-MS: m/z 1433 [$\text{M}]^+$, 1316 [$\text{M} - \text{PEt}_3]^+$. Anal. Found: C, 56.7; H, 6.34; N, 1.00. Calcd for **3**: C, 56.9; H, 6.25; N, 0.98.

Results and Discussion

Similar to the synthesis of complexes **1** and **2**, reaction of the chloroplatinum(II) precursor complex [$\{\text{ClPt}(\text{PEt}_3)_2\text{C}\equiv\text{C}\}_2$ -3,6-*n*BuCarb-9]⁵⁰ with 1-ethynyl-naphthalene in the presence of a catalytic amount of CuCl in HNet₂ and THF afforded complex **3** as a pale orange-yellow solid.⁴⁶ The X-ray crystal structure of complex **3** has been determined. Figure 1 shows the perspective drawing of complex **3**. The structural features of complex **3** are comparable to those in the chloroplatinum(II)

precursor complex [$\{\text{ClPt}(\text{PEt}_3)_2\text{C}\equiv\text{C}\}_2$ -3,6-*n*BuCarb-9].⁵⁰ The bond angles between the alkynyl ligand and the platinum metal centers are in the range of 174.9(12)–177.3(10)° and are close to the ideal of 180° for sp-hybridized carbon, further confirming the σ -bonded nature of the alkynyl groups in these complexes. The slightly longer Pt–C bond distances found in complex **3** (2.012(11)–2.027(13) Å) compared to those in the precursor complex (1.87(3) and 1.97(3) Å) are ascribed to the stronger *trans* influence as a consequence of the presence of the second set of alkynyl groups in the bis(alkynyl) complexes in comparison to that of the chloroplatinum(II) precursor complex. The coordination geometry of complex **3** at the platinum center is essentially square planar with slight distortions, with the P–Pt–C bond angles in the range of 87.9(3)–92.8(3)°, probably due to relief of steric hindrance from the presence of bulky ligands about the platinum(II) metal centers. The coordination planes about each platinum atom in complex **3** are not coplanar with the carbazole backbone, with interplanar angles of 69.1–70.4°, which are similar to those found in the crystal structure of the chloroplatinum precursor.⁵⁰ All the bond distances and angles were found to be normal and are comparable to that found in other related platinum(II) alkynyl complexes.⁴⁶ Selected bond distances and angles are given in Table 1.

The electronic absorption spectra of the complexes are dominated by intense absorption bands at ca. 354–370 nm with extinction coefficients on the order of $10^4 \text{ dm}^3 \text{ mol}^{-1} \text{ cm}^{-1}$. Similar absorption bands with comparable extinction coefficients have been observed for the organic alkynes and the corresponding chloroplatinum(II) precursor complexes, which are suggestive of the largely intraligand (IL) character of these absorption bands. The linear electronic absorption and emission spectra of complexes **1** and **3** are shown in Figure 2, and the corresponding spectral data of complexes **1**–**3** are summarized in Table 2. In view of the observation of slight red shifts of absorption and emission energies on going from the chloropalladium(II) alkynyl complex to its chloroplatinum(II) analogues, the lowest energy absorption bands of these complexes are best described as the $\pi \rightarrow \pi^*$ IL/ $d\pi(\text{Pt}) \pi^*(\text{C}\equiv\text{C})$ MLCT transitions with predominantly IL character.⁴⁷ Upon photoexcitation at $\lambda > 350$ nm, vibronically structured emission bands were observed for complexes **1** (532 nm), **2** (548 nm), and **3** (546 nm) in degassed benzene solutions. The large Stokes shifts and the luminescence lifetimes in the microsecond range are typical of emission origins with triplet parentage. In view of the close resemblance of

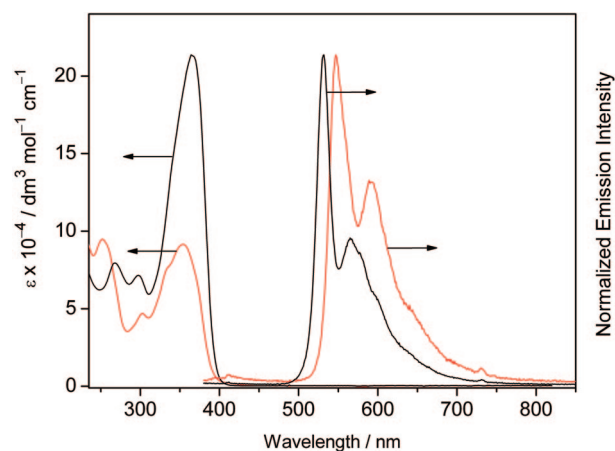


Figure 2. Electronic absorption spectra in dichloromethane (left) and normalized emission spectra in the solid state (right) of complexes **1** (black lines) and **3** (red lines) at room temperature.

Table 2. Linear and Nonlinear Photophysical Data for Complexes 1–3

complex	abs ^a λ/nm (ε/dm ³ mol ⁻¹ cm ⁻¹)	λ _{em} ^b /nm (τ ₀ /μs)		Φ _{em} ^{b,c}	σ ₂ ^b /GM
		λ _{ex} = 355 nm	λ _{ex} = 740 nm		
1	268 (79 610), 298 (71 610), 338 sh (134 590), 364 (213 650)	532 (41.4)	533	0.30	32
2	308 (78 380), 370 (244 950)	546 (68.0)	547	0.31	13
3	252 (94 920), 302 (46 990), 332 sh (74 260), 354 (91 540), 372 sh (66 640), 412 sh (2110)	548 (<0.1)	548	0.19	14

^a In CH₂Cl₂ at 298 K. ^b In benzene at 298 K. ^c Using quinine sulfate in 1.0 N H₂SO₄ as the reference (excitation wavelength 365 nm, Φ = 0.55).⁵⁵

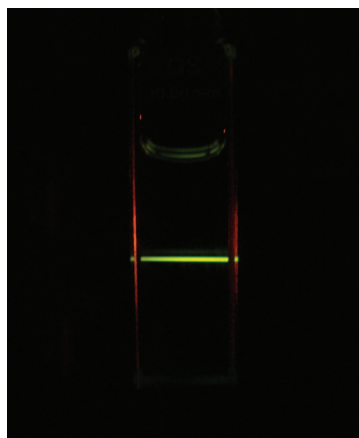


Figure 3. TPIL observed from complex **1** in benzene at a concentration of 1.80×10^{-4} mol dm⁻³ upon excitation with a mode-locked femtosecond Ti:Sapphire laser at 740 nm. The horizontal green line is the TPIL observed from complex **1**, while the red vertical lines are scattered light of the 740 nm excitation laser by the 1 cm quartz cell.

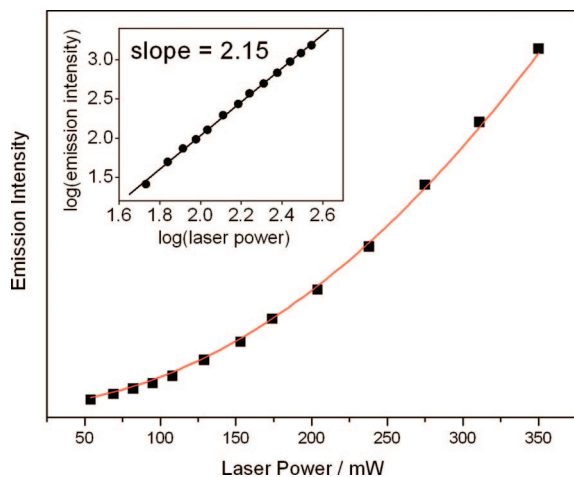


Figure 4. Power dependence of the upconverted luminescence intensity (■) of complex **3** in the thin-film solid state at room temperature. The red line shows the theoretical curve for the quadratic function. The inset shows the log(emission intensity) (●) vs log(laser power) and its linear regression (—).

vibronic structures and emission energies for complexes **2** and **3**, which are different from those of complex **1**, the emissions of complexes **2** and **3** are likely to emanate from similar intraligand triplet excited states that are associated with the naphthyl moieties. Such spin-forbidden transitions are “switched on” due to the strong spin–orbit coupling exhibited by the heavy Pt(PET₃)₂ moieties. However, a red shift in emission energies was observed on going from the palladium alkynyl complexes to their platinum analogues,⁴⁷ which is indicative of some mixing of $d\pi(M) \rightarrow \pi^*(C\equiv C)$ ³MLCT character in the emissive states. Thus, the nearly identical yellow-orange emission bands observed for complexes **2** and **3** are likely to originate

predominantly from the ³IL states of the naphthyl alkynyl moieties with some mixing of $d\pi(Pt) \rightarrow \pi^*(C\equiv CNp)$ ³MLCT character. On the other hand, the yellowish green emission of complex **1** was assigned to be derived from triplet states of the (C≡CC₆H₄C≡C)₃C₆H₃-1,3,5 central core with some mixing of MLCT[$d\pi(M) \rightarrow \pi^*(C\equiv CR)$] character, as the mononuclear complex *trans*-[Pt(PET₃)₂(C≡CC₆H₄CH₃)₂] has been found to emit at shorter wavelength with an emission maximum at ca. 450 nm. The absence of ³IL emissions derived from the central (C≡CC₆H₄C≡C)₃C₆H₃-1,3,5 and (C≡C)₂-3,6-*n*BuCarb-9 moieties in complexes **2** and **3**, respectively, was attributed to the facile energy transfer from the central core to the lower lying excited states associated with the peripheral naphthyl moieties in these multinuclear platinum(II) systems.⁴⁶

Upon excitation by a mode-locked femtosecond Ti:Sapphire laser at 740 nm, complexes **1–3** emit in the green to yellow region both in degassed benzene solutions (concentration $\sim 10^{-5}$ M) and as a thin film in the solid state at room temperature. Figure 3 shows an image of the TPIL observed for complex **1** excited by a mode-locked femtosecond Ti:Sapphire laser at 740 nm. No linear absorption in the wavelength range from 500 to 820 nm was observed for the platinum(II) complexes. The lack of linear absorption in this region implies that the emission induced by 740 nm excitation could not be attributed to a linear process but rather to a nonlinear process. The upconverted emissions of these complexes are nearly identical with those observed in their corresponding single-photon excited emission spectra. The dependence of the upconverted luminescence intensities on the incident laser power was measured, and the power dependence curve for complex **3** in the thin-film solid state is shown in Figure 4. The inset shows the plot of log(emission intensity) vs log(laser power), which gave a straight line with a slope of 2.15. The nearly perfect quadratic dependence and the slope of ca. 2 in the log(emission intensity) vs log(laser power) plot both in degassed benzene solutions in the concentration range 3×10^{-5} – 1×10^{-6} mol dm⁻³ and in the thin-film solid state further confirm the two-photon nature of the process.

The two-photon absorption cross-sections of the complexes could be determined by comparing their two-photon induced luminescence intensity with the two-photon fluorescence excitation cross-section of rhodamine 6G at a concentration of 2.65×10^{-5} mol dm⁻³ as the reference, according to eq 1:

$$\sigma_{2(s)} = \frac{C_r n_r \Phi_r S_r}{C_s n_s \Phi_s S_r} \sigma_{2(r)} \quad (1)$$

where σ_2 is the two-photon absorption cross-section, C is the concentration, n is the refractive index, Φ is the luminescence quantum yield, and S is the integrated luminescence signal. The subscripts r and s refer to the reference and the sample material, respectively. The luminescence quantum yields and two-photon absorption cross-sections of complexes **1–3** are summarized in Table 2. The obtained σ_2 values of these branched multi-

nuclear platinum(II) complexes are about 2–3 times larger than for most other mononuclear platinum(II) complexes that are structurally related to bis((4-(phenylethynyl)phenyl)ethynyl)-bis(tributylphosphine)platinum(II), with reported σ_2 values generally in the range of ~ 5 – 10 GM,^{36–38,40} probably due to the increased number of chromophoric units in the branched complexes. An enhancement in TPA cross-section was noted upon incorporation of the relatively more electron-rich tolyl moieties at the periphery in complex **1** in comparison to the naphthyl moieties in complex **2**. This provides a convenient handle for the enhancement of TPA cross-section by a simple modification of the peripheral substituents. In view of the readily tunable directional energy transfer within different moieties of the molecule, these complexes represent a new class of versatile materials for the preparation of TPIL materials with different emission characteristics.

In summary, multinuclear platinum(II) alkynyl complexes are found to show two-photon absorption and two-photon induced luminescence properties. The substituents of these complexes could be readily modified with electron-donating or -withdrawing substituents, which provides a handle for the perturbation of both the emission energies and TPA cross-sections. Work is in progress to study the structure–property relationship of the

substituents on the two-photon absorption cross-sections and two-photon induced luminescence properties of the platinum(II) alkynyl complexes.

Acknowledgment. V.W.-W.Y. acknowledges receipt of the Distinguished Research Achievement Award from The University of Hong Kong. We also acknowledge support from the University Development Fund and the Faculty Development Fund of The University of Hong Kong, The University of Hong Kong Foundation for Educational Development and Research Limited, and the URC Matching Fund for the Strategic Research Theme on Molecular Materials. The work described in this paper has been supported by a RGC Central Allocation Vote (CAV) Grant (HKU 2/05C). C.-H.T. acknowledges support from the University of Hong Kong and the receipt of a University Postdoctoral Fellowship.

Supporting Information Available: Tables giving crystal data, atomic coordinates, thermal parameters, and all bond distances and angles for complex **3**. This material is available free of charge via the Internet at <http://pubs.acs.org>.

OM800338X